



FULL PAPER

Structural, electronic, and thermodynamic properties of TiO₂/organic clusters: performance of DFTB method with different parameter sets

Vladimir S. Naumov^{1,2} | Anastasiia S. Loginova¹ | Alexander A. Avdoshin¹ |
Stanislav K. Ignatov¹ | Alexey V. Mayorov^{3,4} | Bálint Aradi² | Thomas Frauenheim²

¹Department of Chemistry and Research Institute of Chemistry, N.I. Lobachevsky State University of Nizhny Novgorod, Nizhny Novgorod, Russia

²Bremen Center for Computational Material Studies, University of Bremen, Bremen, Germany

³Mass Spectrometry Data Center, National Institute of Standards and Technologies, Gaithersburg, Maryland

⁴A. A. Kharkevich Institute for Information Transmission Problems, Russian Academy of Sciences, Moscow, Russia

Correspondence

Vladimir S. Naumov, Department of Chemistry and Research Institute of Chemistry, N.I. Lobachevsky State University of Nizhny Novgorod, Nizhny Novgorod, Russia.
Email: vsnaumov@yandex.ru

Funding information

Deutscher Akademischer Austauschdienst; Ministry of Science and Higher Education of the Russian Federation, Grant/Award Number: 0729-2020-0053; Russian Foundation for Basic Research, Grant/Award Numbers: 18-33-00721, 18-43-520012, 20-03-00282

Abstract

The clusters of bare TiO₂ and TiO₂ with linked organic ligands modeling polyorganic composites used as photocatalytic materials were studied using the density functional based tight binding (DFTB) electronic structure method with three parameter sets (*trans3d*, *tiorg*, and *matsci*) in comparison with results of B3LYP/6-31G(d,p) calculations, semiempirical methods PM6 and PM7, and available experimental data. It was found that the highly scalable DFTB method shows results that are close to the B3LYP/6-31G(d,p) level of theory. The corrected version of the *tiorg* DFTB parameter set (*tiorg-smooth*) has better performance for the estimations of structural parameters, whereas the *trans3d* set better reproduces energies of the composite material formation in polycondensation reactions. Performance of the *matsci* set is somehow in the middle of the *tiorg-smooth* and *trans3d* sets. The *tiorg-smooth* and *matsci* sets can be used for the studies of adsorption complexes of bare TiO₂ clusters. All three DFTB parameter sets well estimate the electronic parameters of clusters (HOMO-LUMO gap, ionization potential, and dipole moment). DFTB results are closer to the estimates made with DFT (B3LYP/6-31G(d,p)) than the results of PM6 and PM7 methods. DFTB calculations of large (up to 448 atoms) bare TiO₂ and TiO₂/organic clusters (72 structures in total) confirm the robustness and computational efficiency of the method.

KEYWORDS

clusters, DFT, DFTB, HEMA, parameter sets performance, semi-empirical methods, TiO₂

1 | INTRODUCTION

Titanium oxide is one of the most widely used components of modern materials in the field of photovoltaics and photocatalysis.^[1-3] For such applications, the nanostructured TiO₂ incorporated in the porous polymeric matrices preventing nanoparticle cohesion is considered a promising photocatalytic material for oxidation reactions providing, for example, the efficient elimination of environmental organic contaminants. Its action is based on the formation of Ti³⁺ active centers during the light absorption or by the electron transfer from the neighboring metallic nanoparticles incorporated into the same matrix. This mechanism of action makes the nanomaterial open for further improvements on the basis of quantum chemical modeling of these processes with variation of the cluster size, morphology, and matrix composition. This modeling is, however, complicated by the necessity of carrying out quantum calculations for the large bulks of material with incorporated real-scale nanoparticles because the small models are not representative of the description of the processes occurring on the nano level.

The analysis of studies on the properties of the TiO₂-based nanomaterials shows that the requirements for the minimum cluster size, which would ensure a correct description of these properties, are permanently growing. For instance, one study^[4] reported (TiO₂)₆ as the cluster-reproducing band gap of bulk TiO₂. In a theoretical study,^[5] the authors conclude that (TiO₂)₆ clusters are able to estimate semiquantitatively features of electronic structure of the Ti/alizarin complexes. Later, the same authors^[6] found that (TiO₂)₁₅ is the minimal cluster that could provide a complete picture for the TiO₂/catechol system. Studies^[7,8] show that the (TiO₂)₂₄(OH)₄ cluster could be a reasonable compromise between accuracy and computational costs. One of the most recent studies^[9] systematically focused on Ti_nO_{2n+2}H₄ clusters with *n* from 14 to 54, and the main conclusion is that at least 34 titanium atoms in a cluster are necessary to provide reliable predictions for the photocatalytic and photovoltaic applications. The growth of the minimal cluster size makes DFT calculations that are routinely used for the calculations of reactions between small- and medium-size molecules impractical, and various kinds of simplified quantum chemical methods should be utilized. There are few main approaches to simulate relatively large TiO₂ models. Most of the studies explore large TiO₂ models using B3LYP^[8-17] or Perdew–Burke–Ernzerhof (PBE)^[6,13,18-21] functionals combined with simplified basis sets, including the effective core potentials approach.^[7,10-12,14,15,17] Other studies use semiempirical methods.^[16,22-24] Works using Car-Parinello calculations with plane-wave basis and ultrasoft pseudopotentials should also be noted.^[13,18-20]

Among the variety of simulation methods, the density functional tight-binding theory (DFTB) is one of the promising alternatives. It provides a very efficient estimation of different properties for many organic,^[25-28] inorganic,^[29-32] and organometallic^[33-35] species. However, its application to the TiO₂-based materials, especially in contact with metallic nanoparticles, is still restricted due to the lack of reliable atomic parameters for Ti and other metal atoms. Earlier, several parameter sets were proposed for TiO₂-based materials: *trans3d*,^[36] *tiorg*,^[37] and *matsci*.^[38-41] As noted by the authors of *trans3d* parameters,^[36] there are some known difficulties concerning the Ti–O bond and O–Ti–O angles. The *tiorg* parameter set was developed mostly for the solid-state applications and tested only with small molecular systems.^[37] The *matsci* parameters for Ti were tested mainly for systems comprising Ti, O, and H atoms^[40,41] and for rather specific cases, such as interactions of TiO₂ with phosphonic acids^[38] or DNA.^[39] Modifications of *matsci*—called *matorg* and *matorg + HBD*—should be noted as they show the results close to the DFT level for TiO₂-water systems. However, it is not completely clear how good all these parameter sets are for the description of TiO₂ nanoparticles and clusters incorporated into organic matrix, which form numerous chemical bonds with oxide atoms and modify their electronic properties.

In the present article, we make a systematic comparison between DFTB parameter sets and compare them with the results of the DFT calculations, as well as with available experimental data and calculations performed with semiempirical methods PM6 and PM7, which were successfully used for bare TiO₂ clusters in recent studies.^[16,23,24] The goal of this study is to assess how reliable the estimates made with three DFTB parameter sets are in the small-size and medium-size organo-inorganic clusters and how effective and robust the DFTB calculations of the large-sized TiO₂ clusters are, with the organic ligands modeling real-world organo-inorganic composite materials. Among the properties of interest, we consider the structure of clusters with grafting ligands, their electronic properties (ionization potentials, electron affinities, band gaps, dipole moments), vibrational spectra, and thermodynamic parameters of the composite cluster formation because the proper prediction of these properties are most important for the design and synthesis of the photocatalytic materials.^[42] As an example of the grafting ligands, we consider here the residues of hydroxyethylmethacrylate (CH₂=C(CH₃)–C(O)–O–C₂H₄–OH, HEMA), which was used recently for the synthesis of TiO₂-based nanocomposite materials with improved photocatalytic properties.^[43-45]

2 | COMPUTATIONAL DETAILS

All DFTB calculations were carried out using the DFTB+ code^[46] and three parameter sets elaborated earlier: *trans3d*,^[36] *tiorg*,^[37] and *matsci*.^[38,39] In addition, the *tiorg* parameter set was modified in order to achieve better performance in vibrational frequency calculations of composite materials. This modification includes improved spline smoothing of the Ti–X atomic potentials (where X = C, H, O, Ti). Due to this modification, the non-realistically high vibrational frequencies, which had been found at the organic-inorganic interfaces, were eliminated. Using the modified parameter set (which will be referenced in the following as *tiorg-smooth*), calculations were performed for the whole set of structures. Because the results obtained with *tiorg* and *tiorg-smooth* parameters are essentially the same for all the properties except the vibrational frequencies, we will describe below only the results obtained with the *tiorg-smooth* parameter set. The *tiorg-smooth* parameter set is available for download on the website <http://www.qchem.unn.ru>.

The data calculated using the DFTB method were compared with DFT and semiempirical calculation results. The DFT calculations at B3LYP/6-31G(d,p), CAM-B3LYP/6-31G(d,p), and semiempirical (PM6^[47] and PM7^[48]) theory levels were performed using Gaussian03^[49] and Gaussian16^[50] programs. The DFT functional and basis sets were chosen on the basis of the previous study of the TiO₂/HEMA composites,^[44] where this level of theory was the best among the levels, well reproducing structural, energetic, and electronic parameters of small TiO₂/HEMA clusters, as well as these composites with coordinated Au atoms and clusters.

Structures 1 to 19 (Figure 1) in the DFT calculations were geometrically relaxed at the B3LYP/6-31G(d,p) theory level. For structures 20 to 27, geometries reported by Chen^[16] at the B3LYP/DZVP2 level were taken for the single-point DFT calculations. In addition, for structures 20, 21, and 22, geometry optimization were performed at the B3LYP/6-31G(d,p) level in order to estimate the discrepancies between 6-31G(d,p) and DZVP2. We consider these discrepancies negligible and predictable (see Table 1) and therefore use DZVP2 geometries in the further comparisons

between DFTB, semiempirical, and DFT methods. To estimate electronic properties, CAM-B3LYP/6-31G(d,p) and B3LYP/6-31G(d,p) single-point calculations were carried out with the geometries optimized at the B3LYP/6-31G(d,p) level for the TiO₂/organic clusters and at the B3LYP/DZVP2 level for the bare TiO₂ particles.

The cluster structures chosen for the calculations include several types of structures: (a) the bare clusters with morphology of anatase and rutile crystals, (b) the clusters found earlier to be very favorable at DFT (B3LYP/DZVP2) and PM6 levels,^[16] and (c) the clusters with linked organic ligands. Some of the TiO₂/organic clusters were generated on the basis of recently described structures of TiO₂ particles.^[51,52] Among the organic ligands, the HEMA substituents were used in the most cases as real-world polymers used for the photocatalytic composite synthesis.^[43] The bare TiO₂ structures could also be prospective for photocatalytic activity. For example, structure 25 (ti64a) was noted by the authors as having few potentially active catalytical sites due to structural specificity of surfaces.^[16] For some clusters, the H atoms were used as boundary terminators. All 72 structures were calculated using DFTB with different parameters sets, and 27 of them were studied using DFT, PM6, and PM7 levels of theory. During the geometry optimization, some of starting geometries were analogous to the structures considered in recent studies.^[16,44]

To estimate the adsorption energies of the CO molecule on TiO₂ surface, cluster structures 20 (ti10a), 24 (ti48b), and 25 (ti64a) were used. For each of these bare TiO₂ clusters, six adsorption complexes were considered (three interaction sites in combination with two orientations of

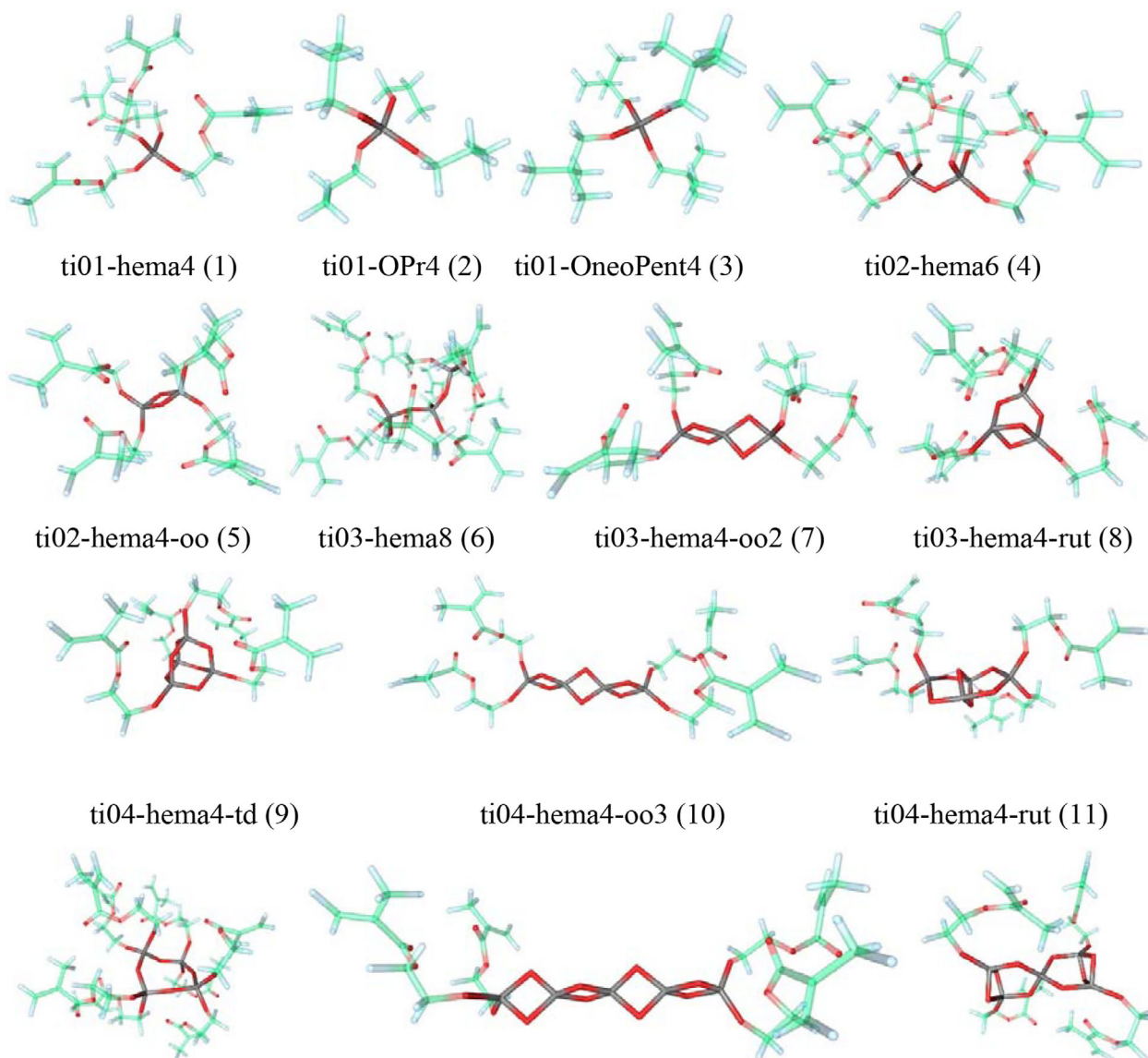
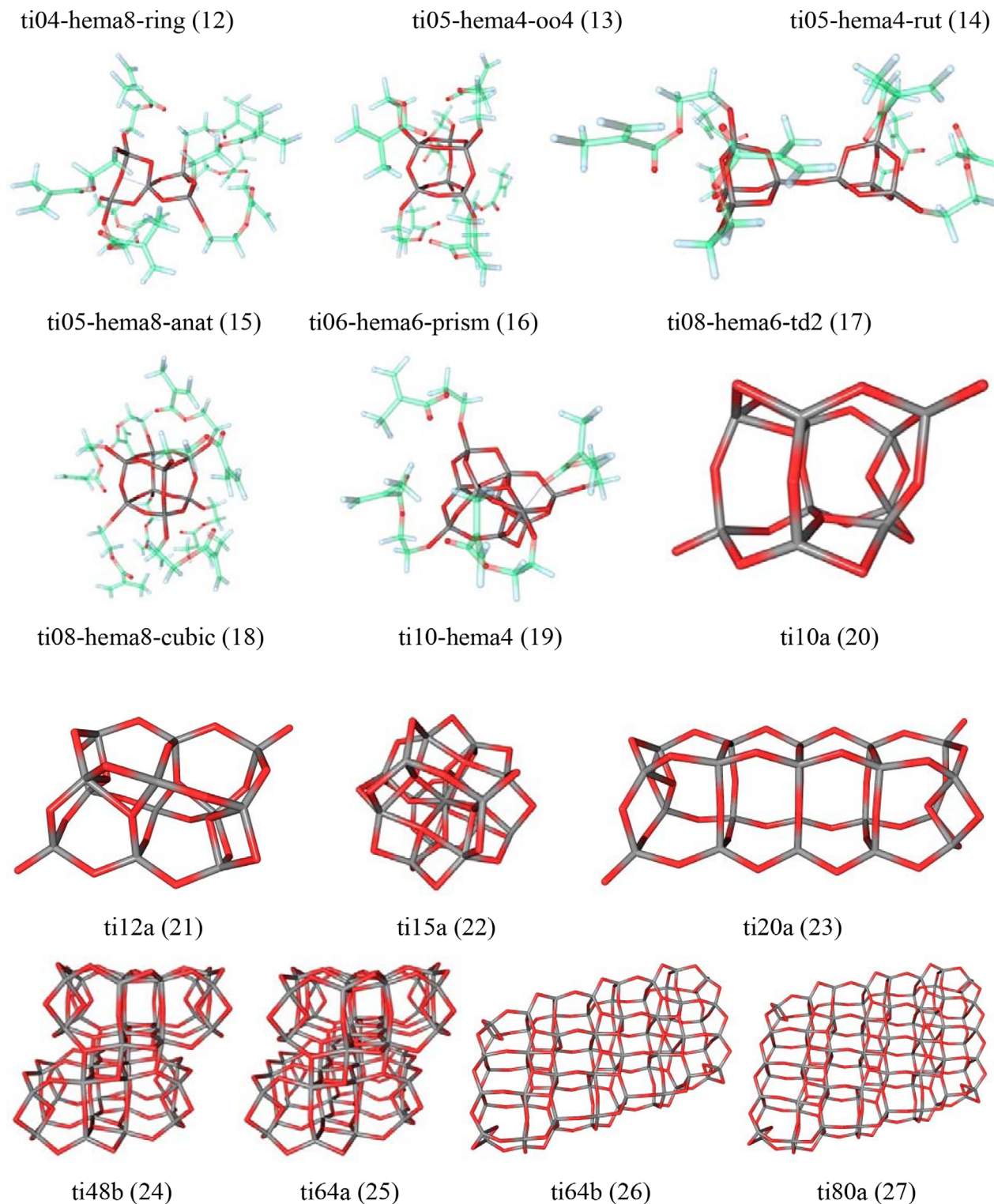


FIGURE 1 Structures of the clusters studied at the DFTB and DFT levels. Structures correspond to the DFT calculation results. The cluster designations represent structure type: numbers after “ti” correspond to the number of Ti atoms, and numbers after “hema”/“OPr”/“OneoPent” correspond to the number of organic residues. In addition, some structural and geometrical motifs in structures 1 to 19 are designated as “oo” for the double-O bridges, “anat” for the anatase motifs, “rut” for the rutile motifs, “cubic”, “prism”, and “td” (tetrahedron). Designations of structures 20 to 27 are the same as in^[16]

**FIGURE 1** (Continued)

CO molecule). Calculations were performed for the on-top complexes when CO is coordinated on a single Ti atom. The initial Ti...C/O distances were about 2 Å. All the adsorption calculations were performed using three DFTB parameter sets: *trans3d*, *tiorg-smooth*, and *matsci*. Some small adsorption complexes were also studied at the B3LYP/6-31G(d,p) level. Some structures optimized with the *tiorg-smooth* parameter set are represented in Figure 2. In addition, combined DFTB calculations with *tiorg-smooth* geometrical preoptimization and further optimization with *trans3d* were performed to estimate the performance of the parameter sets (see further details in the Results section).

TABLE 1 Structural and electronic parameters of the bare TiO₂ clusters at different DFT theory levels

Property	DFT Basis	Structures (Figure 1)		
		10a (20)	12a (21)	15a (22)
Structural properties				
Ti–O, Å (averaged values)	DZVP2 ^a	1.858	1.849	1.899
	6-31G(d,p)	1.843	1.844	1.857
O–Ti–O, ° (averaged values)	DZVP2 ^a	107.3	108.0	106.3
	6-31G(d,p)	107.4	107.8	107.0
Electronic properties				
IP (–E _{HOMO}), eV	DZVP2 ^a	8.75	8.90	8.94
	6-31G(d,p) // DZVP2 ^b	8.51	8.70	8.77
	6-31G(d,p)	8.62	8.80	8.63
EA (–E _{LUMO}), eV	DZVP2 ^a	4.42	4.37	4.41
	6-31G(d,p) // DZVP2 ^b	4.15	4.13	4.23
	6-31G(d,p)	4.05	4.02	3.76
BG, eV	DZVP2 ^a	4.33	4.53	4.54
	6-31G(d,p) // DZVP2 ^b	4.36	4.57	4.54
	6-31G(d,p)	4.57	4.78	4.87

^aData from Reference 16.

^bSingle-point B3LYP/6-31G(d,p) calculations for the geometries from Reference 16.

3 | RESULTS

3.1 | Structural properties

Structures of the clusters calculated at DFT, DFTB, and semiempirical levels are shown in Figure 1. The remaining clusters studied at the DFTB level only within three parameter sets are presented in Figure S1 of Supporting Information. Averaged values of bonds, valence angles, highest occupied molecular orbital (HOMO) and lowest unoccupied molecular orbital (LUMO) energies, and band gaps are represented in Table 2. The data are collected into three groups: (a) the average values among all the structures, (b) the values averaged only among TiO₂/organic clusters, and (c) those only among bare TiO₂ clusters.

According to the available experimental data, average Ti–O bond lengths between the nearest atoms inside the 30 Å nanoparticles are about 1.84 Å for the surface bonds and 1.99 Å for the internal ones.^[51] When the size of the nanoparticles decreases to 19 Å, the average Ti–O bond length reduces to 1.77 Å (surface bonds) and 1.94 Å (internal bonds).^[53] The average Ti–O bond length of bulk TiO₂ crystalline phases is 1.96 Å.^[54,55] As is evident from Table 2, the B3LYP-calculated values are in agreement with experimental data, and the B3LYP values are rather reliable in describing the structure of titanium dioxide.

Statistical analysis of bond lengths and valence angles demonstrates rather significant discrepancies between *trans3d*, *tiorg-smooth*, *mtsci*, DFT, and semiempirical calculated structural parameters. Figure 3 shows the comparison between the mean values of the Ti–O bond lengths, including separate analysis of different types of such bonds: Ti–O_{ino} for oxygen atoms inside the inorganic part of cluster (connected with two titanium atoms) and Ti–O_{org} for oxygen atoms that are connected to titanium and carbon.

Figure 3 shows that calculated bond lengths obtained with DFTB are typically closer to the DFT results than that obtained by the PM6 and PM7 methods. Typical mean absolute deviation (MAD) between DFT and semiempirical levels is up to 0.07 Å. The *trans3d* parameters tend to slightly overestimate the Ti–O bond lengths relative to DFT, especially in the case of Ti–O_{org} moieties (MAD is 0.031 Å). The *tiorg-smooth* parameter set underestimates Ti–O bond lengths by only about 0.001 to 0.003 Å on average, and MAD is up to 0.023 Å and is larger for the TiO₂/organic clusters. In geometries obtained by calculations with *matsci* parameters, the Ti–O bond is overestimated by about 0.021 Å for Ti–O_{ino} (MAD is 0.023 Å); in the case of bonds between organic and inorganic parts, average overestimation is 0.048 Å. Table 3 gives the complete statistical analysis for the discrepancies between DFTB *tiorg-smooth*, DFTB *trans3d*, DFTB *matsci*, PM6, and PM7 in comparison with DFT theory, along with different properties including structural, electronic, and thermodynamic characteristics.

Figure 4 demonstrates the deviations of the O–Ti–O average angles calculated at the DFT, semiempirical, and DFTB levels with *trans3d*, *tiorg-smooth*, and *matsci* parameters. All the methods give quite close results, and MAD from the DFT level is not larger than 1.68°. There are some noticeable exceptions—few structures show the deviations from DFT by about 2 to 3°, which is still a very accurate result. The closest to B3LYP results were obtained by DFTB *tiorg-smooth* (typical MAD value is 0.31°).

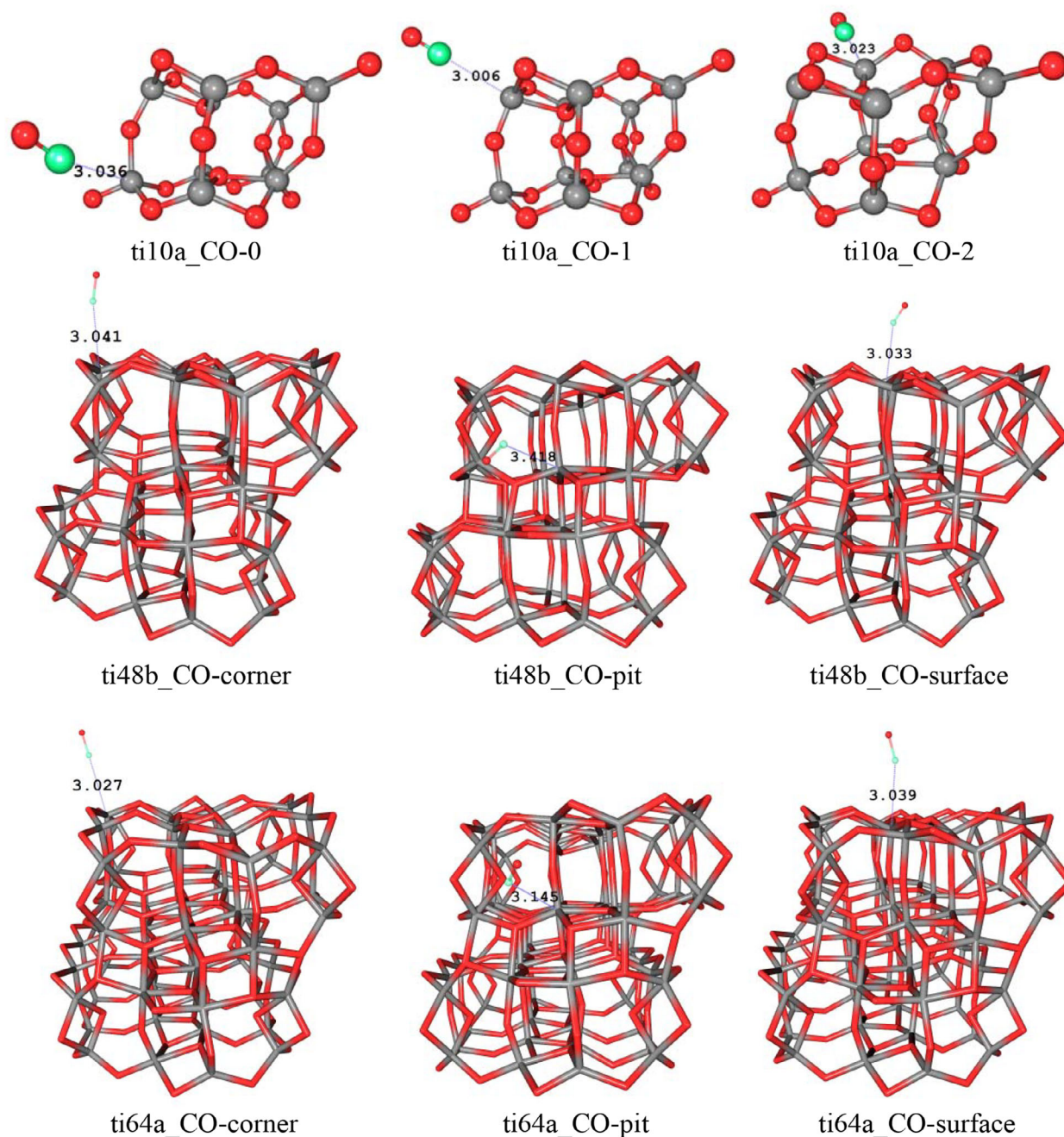


FIGURE 2 Structures of adsorption complexes of carbon monoxide on bare TiO₂ clusters with Ti···C interactions optimized at DFTB *tiorg-smooth* level

The comparison between Ti-O-C angles calculated with different theory levels is shown in Figure 5. As is seen, there are crucial differences between the results of DFT, DFTB, and semiempirical methods. The *tiorg-smooth* demonstrates only negligible deviation from the DFT values (about 140°), whereas other DFTB parameter sets and semiempirical methods give quite unrealistic values of Ti-O-C valence angles of about 115° and 175°, respectively, for all the compounds. These results lead to a significant difference in the MADs as is evident from Table 3: 3.4° for *tiorg-smooth*; 13.9° for *matsci*; and about 30° for *trans3d*, PM6, and PM7.

Based on the results obtained, we conclude that *tiorg-smooth* parameters better describe the bond lengths in the clusters of interests and coincide much better with the DFT values of Ti-O-C valence angles in the organic ligands linked to the TiO₂ surface. All DFTB parameter sets demonstrate good agreement with DFT for O-Ti-O angles. In general, the DFTB method is superior in describing the structure of TiO₂/organic clusters than semiempirical methods.

TABLE 2 Structural and electronic parameters of TiO₂/organic clusters calculated with different quantum chemical methods. Data represent the values averaged among all clusters, among TiO₂/organic clusters (in parentheses), and among bare TiO₂ clusters [in brackets]

Property	DFT	PM6	PM7	DFTB (tos)	DFTB (t3d)	DFTB (mtsc)	Experiment	Exp. Ref.
Structural properties								
Ti–O, Å	1.833 (1.818) [1.869 ^a]	1.874 (1.859) [1.908]	1.869 (1.858) [1.893]	1.831 (1.816) [1.866]	1.849 (1.836) [1.877]	1.859 (1.852) [1.875]	–	
Ti–O _{ino} , Å	1.844 (1.831) [1.869 ^a]	1.897 (1.889) [1.913]	1.900 (1.902) [1.896]	1.841 (1.829) [1.866]	1.852 (1.840) [1.877]	1.865 (1.854) [1.887]	1.959 1.84 / 1.99 1.77 / 1.95	[54,55] [51] [53]
Ti–O _{org} , Å	(1.803) 108.4	(1.814) 109.2	(1.797) 108.5	(1.802) 108.6	(1.834) 109.0	(1.851) 108.4	–	
O–Ti–O, °	(108.8) [107.4 ^a]	(109.2) [109.0]	(108.6) [108.3]	(109.0) [107.4]	(109.0) [109.1]	(108.6) [107.7]	81.12 108.0	[54] [55]
Ti–O–C, °	(143.8)	(176.4)	(172.5)	(141.1)	(112.3)	(129.9)	–	
Electronic properties								
IP (–E _{HOMO}), eV	7.34 ^b /8.97 ^c (6.84 ^b /8.45 ^c) [8.52 ^a /10.19 ^c]	10.65 (10.42) [11.22]	9.70 (9.69) [9.71]	5.78 (5.67) [6.04]	5.91 (5.72) [6.38]	5.99 (5.94) [6.11]	7.96 ^d 7.40 ^e 7.2 ^f 5.17 ^f	[56] [56] [27,57] [58]
EA (–E _{LUMO}), eV	2.48 ^b /1.19 ^c (1.79 ^b /0.47 ^c) [4.12 ^a /2.90 ^c]	1.85 (1.58) [2.49]	1.26 (0.83) [2.29]	2.29 (2.04) [2.90]	2.76 (2.55) [3.31]	2.65 (2.53) [2.95]	4.0 ^f 1.5 ... 3.3 ^g 3.00 ... 3.6 ^g	[57] [59] [4]
BG, eV	4.86 ^b /7.78 ^c (5.05 ^b /7.98 ^c) [4.41 ^a /7.30 ^c]	8.80 (8.84) [8.72]	8.44 (8.86) [7.43]	3.48 (3.63) [3.14]	3.14 (3.17) [3.06]	3.34 (3.42) [3.16]	3.2 ^f 3.23 ^d >3.40 ^d 3.13 ^d 3.06 ^e	[57,58] [60] [60] [61] [61]

Abbreviations: *tos*, *tiorg-smooth* parameter set; *t3d*, *trans3d* parameter set; *mtsc*, *matsci* parameter set.

^aSingle-point B3LYP/6-31G(d,p) with the geometries from Reference 16.

^bB3LYP/6-31G(d,p).

^cCAM-B3LYP/6-31G(d,p).^[69]

^dAnatase.

^eRutile.

^fAmorphous, mixed, or nonspecified phase.

^gTiO₂ clusters.

3.2 | Electronic properties

The main electronic properties regarding the photocatalytic applications are ionization potentials (IPs), electron affinities (EAs), and HOMO-LUMO band gaps (BGs). The latter parameter influences the photoexcitation abilities of the material, whereas the two others affect the ability to accept or donate electrons from/to the “antenna” nanoparticles (of Au, Ag, or other metals) during their photoexcitation. Typically, the Au or other metallic nanoparticles embedded into the composite material enhance the light absorptions due to their plasmon resonance ability and donate electrons to the neighboring TiO₂ particles forming the Ti³⁺ centers.

Although the accurate estimation of vertical ionization potentials and, especially, the electron affinities is a rather complicated task, these properties could be crudely estimated using the Koopmans theorem. Therefore, in this study, we estimated the IP, EA, and BG values using the approximate expressions:

$$IP = -\epsilon_{HOMO}, \quad EA = -\epsilon_{LUMO}, \quad BG = \epsilon_{LUMO} - \epsilon_{HOMO}.$$

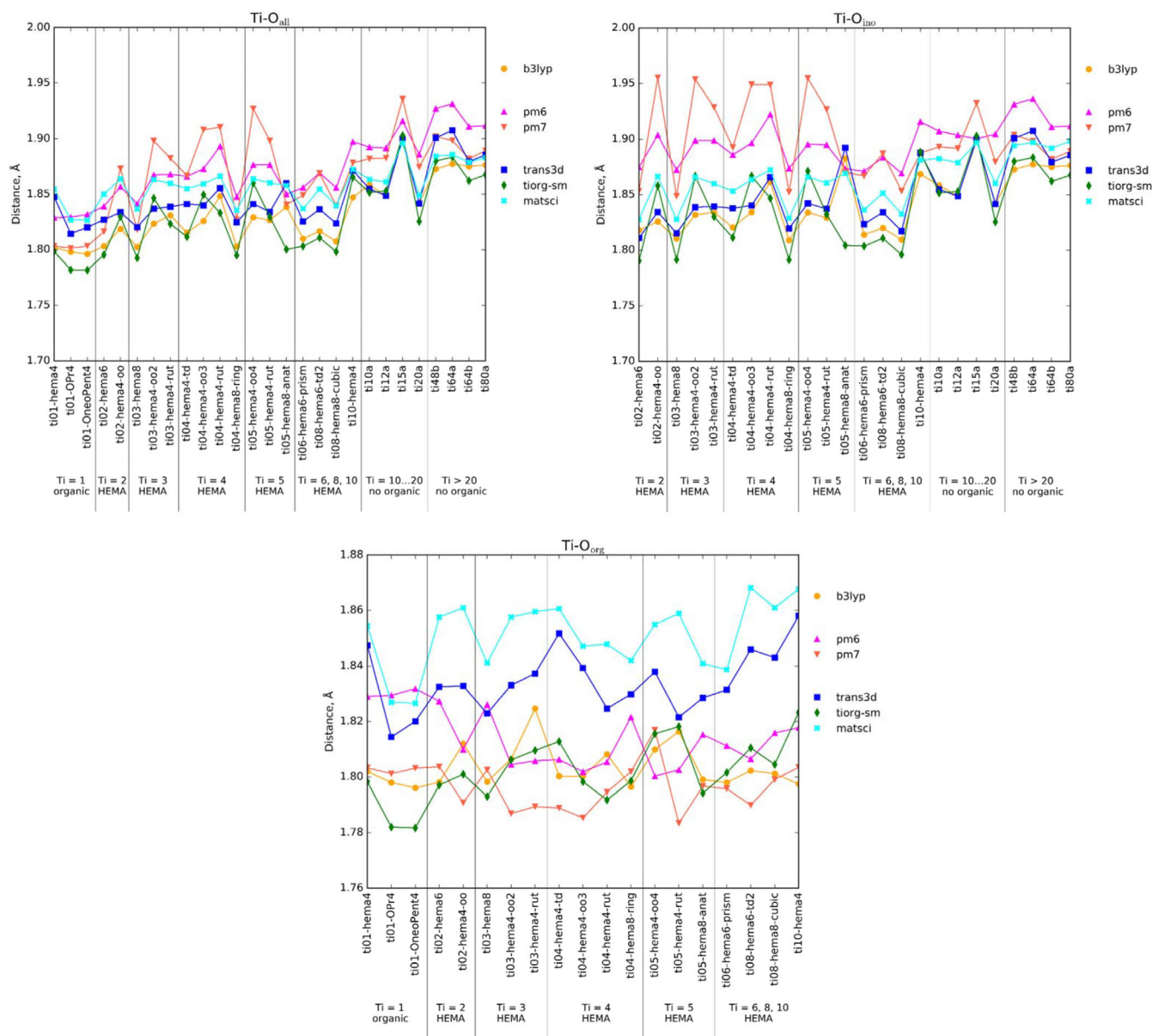


FIGURE 3 The Ti–O bond length values calculated with DFTB and semiempirical methods in comparison with DFT results

One of the most recent studies^[57] discusses the positions of conduction band and oxygen vacancy, and the authors conclude that the earlier^[58] reported value of the ionization potential is not correct due to oxygen vacancy level within the BG. Nevertheless, the value of 5.17 eV reported in^[58] is considered one of the reliable ones. According to some experimental data, including studies of electronic properties of $(\text{TiO}_2)_n$ (where n is up to 10),^[4,59] clusters larger than $(\text{TiO}_2)_6$ could represent electronic properties of bulk titanium dioxide.^[4] At the same time, one theoretical study^[9] reports the $\text{Ti}_{34}\text{O}_{70}\text{H}_4$ cluster as the smallest one, which could reproduce features of electronic properties. Unfortunately, the computational costs of B3LYP/6-31G(d,p) calculations $(\text{TiO}_2)_n/\text{HEMA}$ clusters with $n > 10$ make such calculations impractical.

Values of the HOMO and LUMO energies calculated with DFT and DFTB methods for different cluster types are shown in Figure 7 in comparison with ranges of experimental IPs and EAs. As is evident from the figure, all the methods, including all DFTB parameter sets, demonstrate similar performance for the LUMO energies and reproduce the tendency of EA growth when the cluster size increases in agreement with the results reported earlier.^[4] The common tendency is shifting up of the HOMO and LUMO energy levels in cases with the presence of organic ligands. This effect is more pronounced in the case of DFT calculations where the shift is of about 2 eV. Structures 19 (ti10-hema4) and 20 (ti10a) represent the same TiO_2 cluster structure with and without four HEMA ligands. Analysis of the differences between HOMO and LUMO levels for these structures could generally characterize the influence of organic ligands. As is evident from Figure 6, the frontier orbital shift for DFTB is remarkably lower than in the case of DFT calculations.

TABLE 3 Statistical analysis of the deviations between the results of different methods

Property	Mean deviation						Mean absolute deviation					
	CAM	PM6	PM7	DFTB (tos)	DFTB (t3d)	DFTB (mtsc)	CAM	PM6	PM7	DFTB (tos)	DFTB (t3d)	DFTB (mtsc)
Structural properties												
Ti–O, Å	–	0.041 (0.041) [0.040]	0.036 (0.040) [0.025]	–0.002 (–0.002) [–0.003]	0.015 (0.018) [0.009]	0.026 (0.034) [0.006]	–	0.041 (0.041) [0.041]	0.036 (0.040) [0.025]	0.012 (0.013) [0.008]	0.016 (0.018) [0.010]	0.026 (0.034) [0.007]
Ti–O _{ino} , Å	–	0.053 (0.058) [0.045]	0.056 (0.070) [0.028]	–0.003 (–0.003) [–0.003]	0.008 (0.008) [0.009]	0.021 (0.022) [0.019]	–	0.054 (0.059) [0.045]	0.057 (0.072) [0.028]	0.018 (0.023) [0.008]	0.009 (0.009) [0.010]	0.023 (0.024) [0.019]
Ti–O _{org} , Å	–	(0.011)	(–0.007)	(–0.001)	(0.031)	(0.048)	–	(0.016)	(0.011)	(0.008)	(0.031)	(0.048)
O–Ti–O, °	–	0.76 (0.39) [1.62]	0.08 (–0.25) [0.85]	0.16 (0.20) [0.04]	0.63 (0.19) [1.68]	–0.04 (–0.19) [0.30]	–	0.76 (0.40) [1.62]	0.60 (0.49) [0.85]	0.31 (0.35) [0.22]	0.81 (0.45) [1.68]	0.47 (0.53) [0.33]
Ti–O–C, °	–	(32.6)	(28.6)	(–2.6)	(–31.5)	(–13.9)	–	(32.6)	(28.6)	(3.4)	(31.5)	(13.9)
Electronic properties												
E _{HOMO} , eV	–1.63 (–1.61) [–1.67]	–3.32 (–3.58) [–2.69]	–2.36 (–2.85) [–1.19]	1.56 (1.17) [2.48]	1.43 (1.12) [2.14]	1.35 (0.90) [2.41]	1.63 (1.61) [1.67]	3.32 (3.58) [2.69]	2.36 (2.85) [1.19]	1.56 (1.17) [2.48]	1.43 (1.12) [2.14]	1.35 (0.90) [2.41]
E _{LUMO} , eV	1.29 (1.32) [1.22]	0.63 (0.21) [1.62]	1.22 (0.96) [1.83]	0.19 (–0.25) [1.21]	–0.30 (–0.76) [0.80]	–0.17 (–0.74) [1.17]	1.29 (1.32) [1.22]	0.66 (0.25) [1.62]	1.23 (0.98) [1.83]	0.62 (0.38) [1.21]	0.78 (0.77) [0.80]	0.87 (0.74) [1.17]
BG, eV	2.92 (2.93) [2.89]	3.94 (3.79) [4.32]	3.58 (3.81) [3.02]	–1.38 (–1.42) [–1.27]	–1.72 (–1.88) [–1.34]	–1.52 (–1.63) [–1.24]	2.92 (2.93) [2.89]	3.94 (3.79) [4.32]	3.58 (3.81) [3.02]	1.38 (1.42) [1.27]	1.72 (1.88) [1.34]	1.52 (1.63) [1.24]
μ, D	–	(0.96)	(2.11)	(0.22)	(0.21)	(0.23)	–	(3.57)	(3.20)	(1.51)	(1.88)	(1.92)
Thermodynamic properties												
Δ _r E, kcal/mol	–	(109.6)	(30.0)	(19.5)	(–3.1)	(11.3)	–	(109.6)	(30.0)	(19.5)	(7.4)	(11.3)
Δ _r E per Ti–O bond, kcal/mol	–	(8.8)	(2.0)	(1.3)	(–0.3)	(0.7)	–	(8.8)	(2.0)	(1.3)	(0.6)	(0.7)

Note: Data represent values averaged among all clusters, among TiO₂/organic clusters (in parentheses), and among bare TiO₂ clusters [in brackets]. The least deviations marked with bold font. The reference method is B3LYP/6-31G(d,p). The reference geometries for bare TiO₂ clusters are taken from Reference 16, calculated at B3LYP/DZVP2 level.

Abbreviations: *tos*, *tiorg-smooth* parameter set; *t3d*, *trans3d* parameter set; *mtsc*, *matsci* parameter set; CAM, CAM-B3LYP/6-31G(d,p); μ, dipole moment; Δ_rE, energies of reaction (1).

HOMO energies obtained by DFTB are typically higher than the B3LYP values, and absolute deviations are in ranges of 0.90 to 1.17 eV (TiO₂/organic) and 2.14 to 2.48 eV (bare TiO₂). The *matsci* set shows values closest to the B3LYP average values along all the structures (MAD is 1.35 eV). While DFTB and DFT methods reproduce experimental values quite well, semiempirical methods obviously underestimate the HOMO energies. PM6 typically deviates from DFT by of 2.69 to 3.58 eV depending on the presence of organic ligands (the deviation is lower for the bare TiO₂ clusters). Results obtained with PM7 are closer to the experiment and DFT/DFTB methods than for PM6, but HOMO energy remains underestimated. It should also be noted that, in the case of the bare TiO₂ clusters, PM7 (MAD is 1.19 eV) is closer to B3LYP than DFTB calculations (MAD is in range from 2.14 to 2.48 eV).

Semiempirical methods tend to overestimate LUMO energy. It was found that the older PM6 method is somewhat better in describing this property than PM7. The mean deviation from DFT is different for clusters with and without organic ligands and is larger for the last ones (up to 1.83 eV in case of PM7 calculations). All DFTB parameter sets are closer to B3LYP than the semiempirical methods, and *tiorg-smooth* gives the closest values to the B3LYP result among all the methods (MAD along all the structures is 0.62 eV). It should be noted that most of the LUMO energies obtained by DFTB falls into the range of experimental data, while many of the values obtained by other methods go over the experimental region, especially in the cases of PM7 and CAM-B3LYP for the TiO₂/organic clusters.

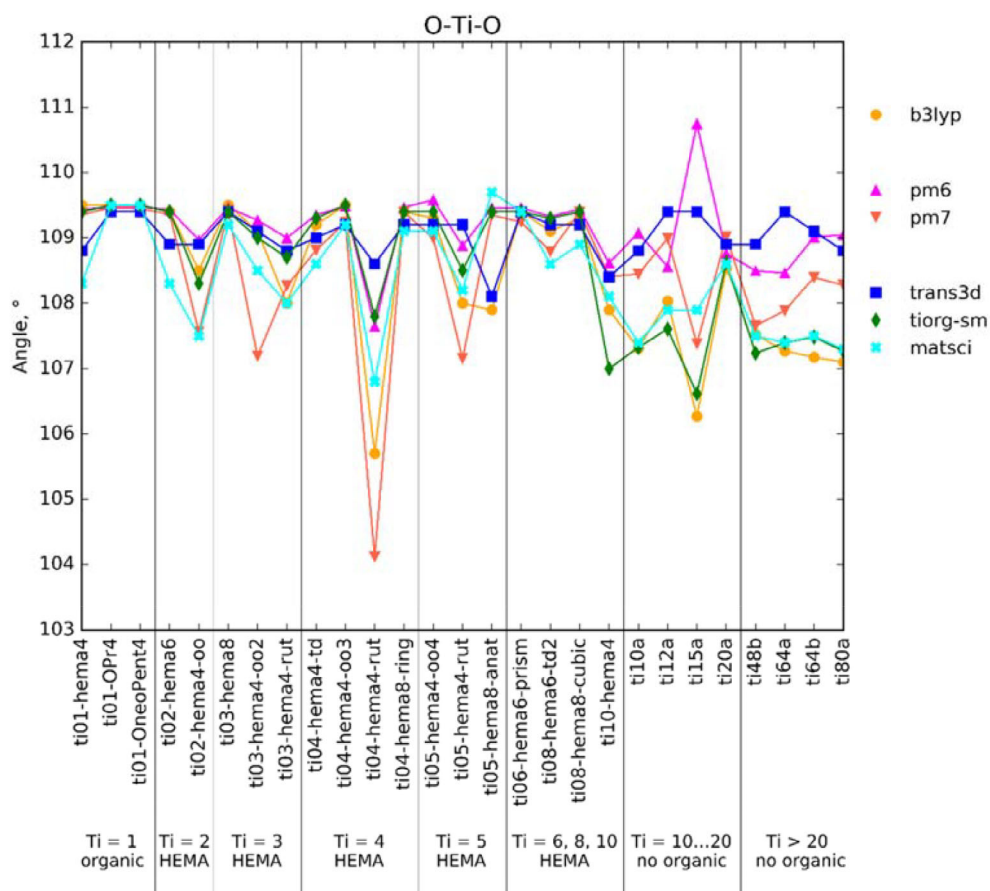


FIGURE 4 The average O—Ti—O valence angles calculated with DFTB and semiempirical methods in comparison with the DFT calculated values

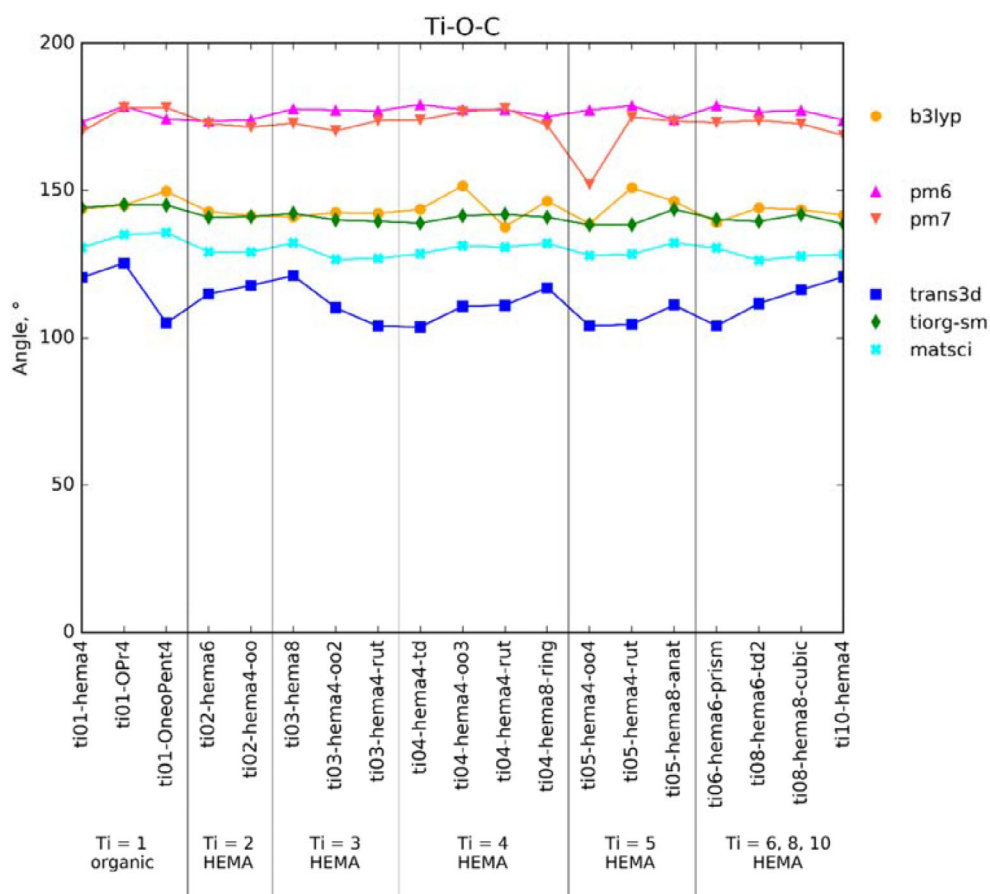


FIGURE 5 The Ti—O—C valence angles calculated with DFTB and semiempirical methods in comparison with the DFT calculated values

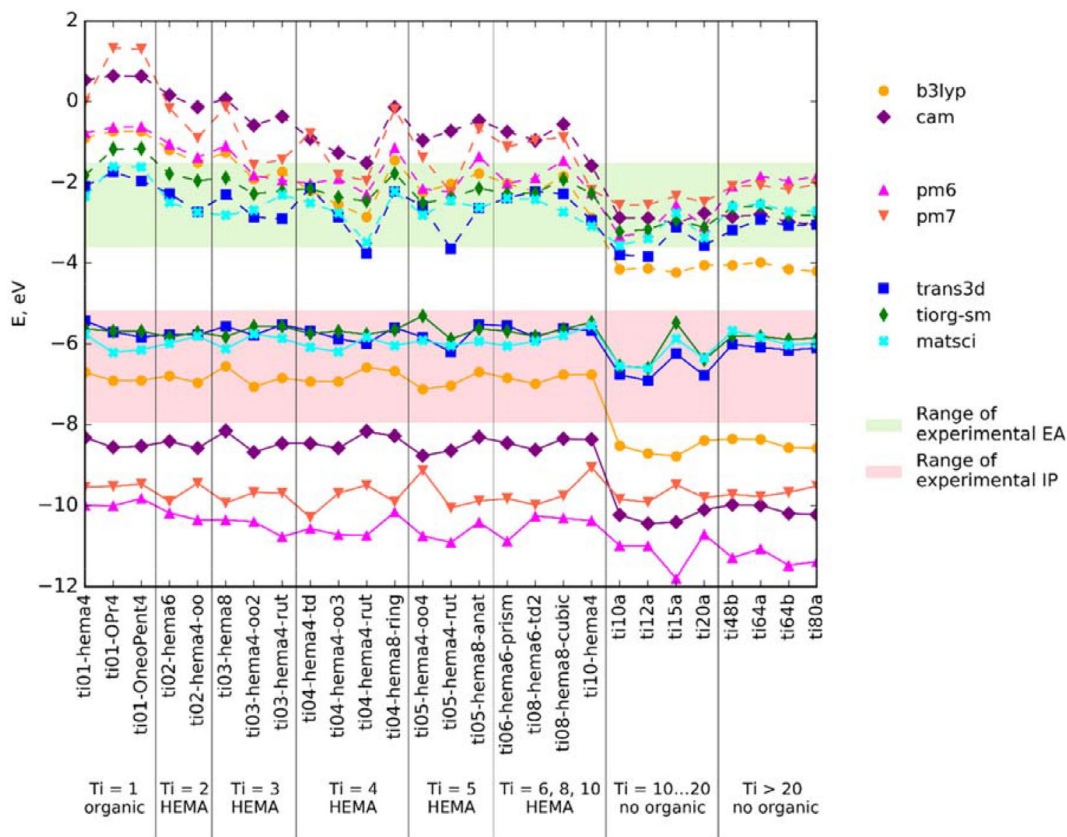


FIGURE 6 HOMO (solid lines) and LUMO (dashed lines) energies obtained by different quantum chemical methods in comparison with ranges of experimental data

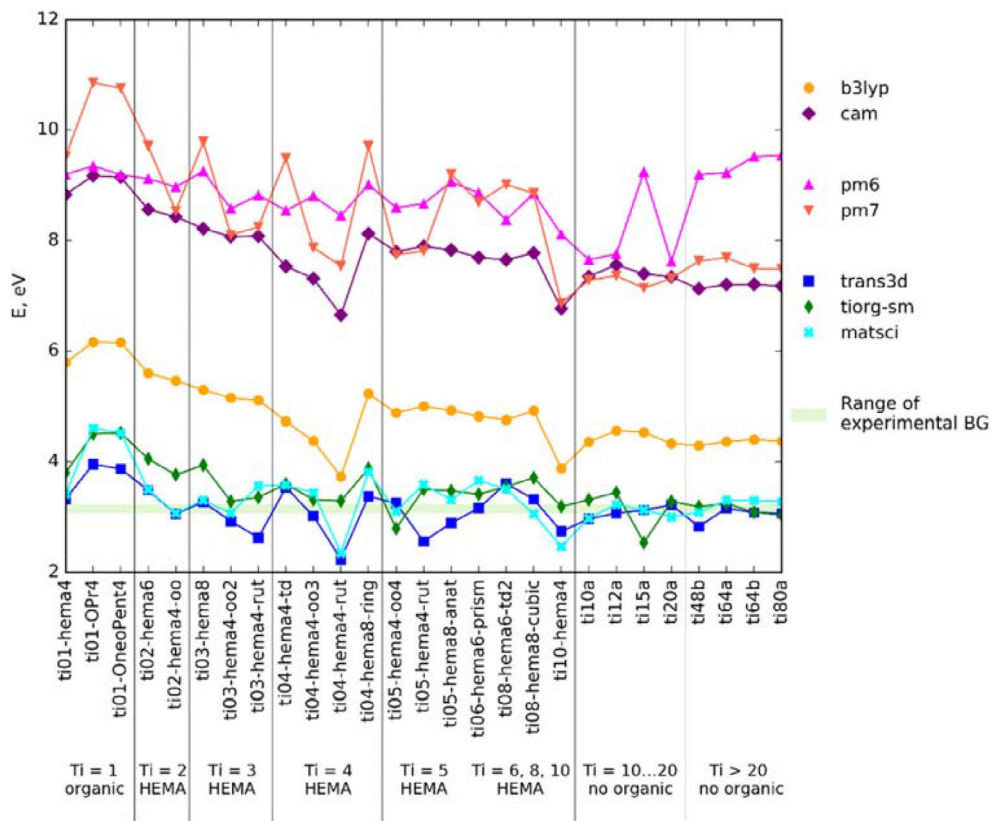


FIGURE 7 Band gaps of the TiO₂/organic and bare TiO₂ clusters obtained by different methods and range of typical experimental values

Average HOMO-LUMO BGs obtained by DFTB are 3.48 eV for *tiorg-smooth*, 3.34 eV for *matsci*, and 3.14 eV for *trans3d*. It is close to the typical experimental values that are in range of 3.03 to 3.23 eV. One of the studies^[60] reports a BG larger than 3.40 eV for anatase particles of titanium dioxide, but authors characterize these results as “unrealistic”. B3LYP gives a BG of about 4.86 eV, higher than experimental values. PM6, PM7, and CAM-B3LYP strongly overestimate the BG by more than 5 eV, and values obtained by these methods are 8.80, 8.44, and 7.98 eV, respectively. Figure 7 shows the calculated BGs of the considered TiO₂/organic and bare TiO₂ clusters in comparison with the range of typical experimental data.

Dipole moment calculations for the TiO₂/organic clusters show that semiempirical methods and DFTB overestimate the absolute value of the dipole moment in comparison with B3LYP. The dipole moments for 19 clusters of TiO₂/organic are represented in Figure 8. The DFTB *tiorg-smooth* method deviates from DFT by 1.51 D and typically works better than *trans3d* (MAD is 1.88 D) and *matsci* (MAD is 1.92 D). The highest deviation from DFT was obtained in the case of PM6 with an MAD of 3.57 D.

3.3 | Vibrational frequencies and IR spectra

The standard DFTB+ software package does not allow direct calculations of IR spectra. However, vibrational frequencies, normal mode coordinates, and dipole moment derivatives can be extracted from the standard DFTB output. The IR spectra could be easily calculated using the simplified formula connecting intensity and dipole moment.^[62] The corresponding python script for such treatment is available in Supplementary Information. The spectra calculated with three DFTB parameter sets for four TiO₂/HEMA structures are represented in Figure 9 in a form of Gaussian envelopes calculated with the following formula:

$$I(\nu) = \frac{\sqrt{\pi}}{\sigma} \sum_i I_i \cdot \exp\left(-\frac{(\nu - \nu_i)^2}{\sigma^2}\right)$$

where I and ν are intensity and wavelength, respectively; I_i and ν_i are the DFTB-calculated intensity and wavelength for mode i , respectively; and σ are the broadening parameters equal to 30 cm⁻¹.

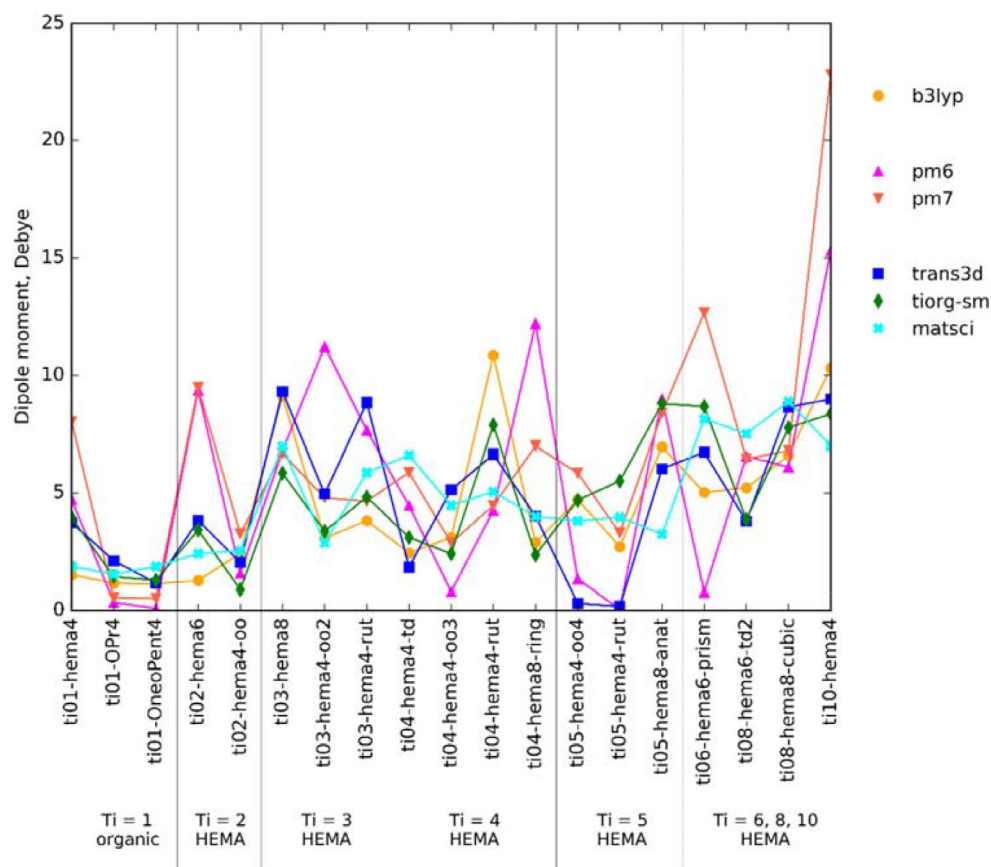


FIGURE 8 Dipole moments of TiO₂/organic clusters obtained by different methods

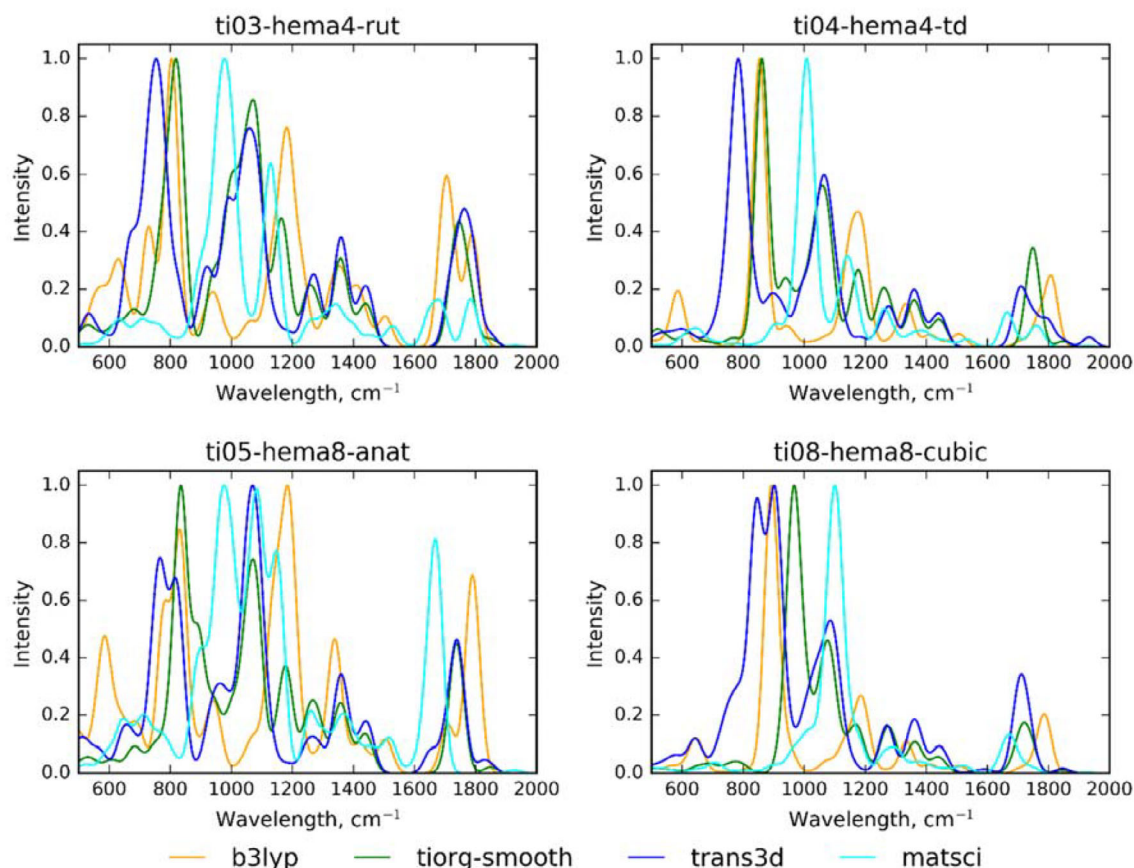


FIGURE 9 IR spectra of some cluster representatives obtained with DFT and DFTB methods

Due to the approximate character of the IR intensity calculations, absolute values of intensities differ significantly between different calculation methods. To eliminate this effect, the intensities were scaled and plotted in arbitrary units to achieve similar peak intensities.

As is evident from the figure, the DFTB spectra calculated with *trans3d* and *tiorg-smooth* parameter sets coincide rather well with the DFT and with each other in the ranges of 700 to 900 cm^{-1} and 1700 to 1900 cm^{-1} . The coincidence in the region of wavelengths of the range 1000 to 1500 cm^{-1} is worse. The vibration assignments in the region between 700 and 1500 cm^{-1} are extremely complicated due to mixing of different vibrational modes. Most of the modes in this region are the complex deformations of organic ligands. There are remarkable admixtures of inorganic part vibrations, both deformational and valence, in the region up to 1000 cm^{-1} . Bands in the range of 1700 to 1900 cm^{-1} mostly correspond to the stretching modes of C=O and C-C bonds. As a whole, the common picture of IR band assignments is reproduced at the DFTB level using *trans3d* and *tiorg-smooth* parameters despite these parameters not being in perfect agreement with DFT in the region of 1000 to 1500 cm^{-1} . As for the *matsci* parameter set, the main difference with DFT is shifting strong peaks from 800 cm^{-1} to 1000 cm^{-1} and the discrepancies in intensity of peaks of around 1600 to 1800 cm^{-1} . It should be noted that the coincidence of semiempirical results (not shown here to make the figure simpler) with DFT is also strongly imperfect. In general, the agreement between DFTB and DFT or experimental spectra is better or at least not worse than when it takes place for the semiempirical methods. The full set of pictures is given in Supporting Information.

3.4 | Cluster formations energies

The properties of fundamental importance in composite material chemistry are the nanoparticle structure, the structural parameter distributions within the partially disordered material, and the distances between nanoparticles. All these characteristics are extremely dependent on the synthesis method, temperature conditions, and time of synthesis. However, one can propose, as a first approximation, that the predominance of various material structures and its phase content are closely connected to the thermodynamic characteristics of the phases formed during the synthesis. This is demonstrated by the time dependence of the formation enthalpy measured during the TiO_2 -based composite synthesis observed experimentally.^[63] It was shown that the changes in the material structure are connected to the enthalpy changes measured at different synthesis phases. Thus, the energy of cluster formation is one of the key properties governing the material structure and compositions. Earlier, it

was found^[44] that, from a thermodynamic point of view, one of the most favorable processes during the synthesis could be represented by the reaction (1):



Here, Pr is *n*-C₃H₇; R is CH₂=C(CH₃)-C(O)-O-C₂H₄- (ie, HEMA); X is TiO₂/HEMA cluster; and *x*, *a*, *b*, *c* are stoichiometric coefficients depending on composition of X.

The energy of this reaction was calculated for the clusters described above. Figure 10 demonstrates a comparison between the reaction energies calculated with different methods. As is evident from the figure, the PM6 method tends to strongly overestimate the reaction energy in comparison with the DFT values. MAD from the DFT values for PM6 is 109.6 kcal/mol (8.8 kcal/mol per Ti-O bond). The overestimation is lower for PM7, which shows a MAD of 30.0 kcal/mol (2.0 kcal/mol per Ti-O bond). Typically, the largest differences are found for the small clusters with five titanium atoms or less. For some of the smallest structures, deviations between B3LYP and PM6 are more than 150 kcal/mol. Deviations decrease for the larger clusters.

DFTB with *tiorg-smooth* parameters also overestimate the energy of cluster formation by about 19.5 kcal/mol (1.3 kcal/mol per Ti-O bond), which is noticeably smaller than the deviation of PM6. A slightly smaller overestimation (about 11.3 kcal/mol or 0.7 kcal/mol per Ti-O bond) of cluster energy formation is also typical for the *matsci* parameter set. DFTB with *trans3d* parameters gives the smallest MAD of 7.4 kcal/mol (0.6 kcal/mol per Ti-O bond) but tends to underestimate the energy of the reaction. At the same time, one of the *trans3d* values (structure 4 or ti02-hema4-oo) deviates from B3LYP by 37.5 kcal/mol (4.7 kcal/mol per Ti-O bond). Exclusion of structure 4 (ti02-hema4-oo) from the cluster set reduces the B3LYP-*trans3d* deviation to 5.4 kcal/mol (0.3 kcal/mol per Ti-O bond).

Both DFTB parameter sets *tiorg-smooth* and *trans3d* use *mio* parameters^[64] for purely organic compounds and give the same energies for the reaction participants that do not contain Ti atoms. The source of the discrepancies between *tiorg-smooth* and *trans3d* could be the Ti atom parameters or the Ti-X bond parametrization (X = C/O/H/Ti). Because the HOMO/LUMO levels are reproduced well within both parameter sets, the main source of the above discrepancies is caused by the Ti-X repulsive interactions, which were fitted in these two sets using different reference systems and quantities. In the *tiorg-smooth* parameter set, the emphasis was mostly on the solid-state energy parameters and the band structure rather than on the thermodynamic properties of complex clusters. The energies of organic components obtained by DFTB with the *matsci*

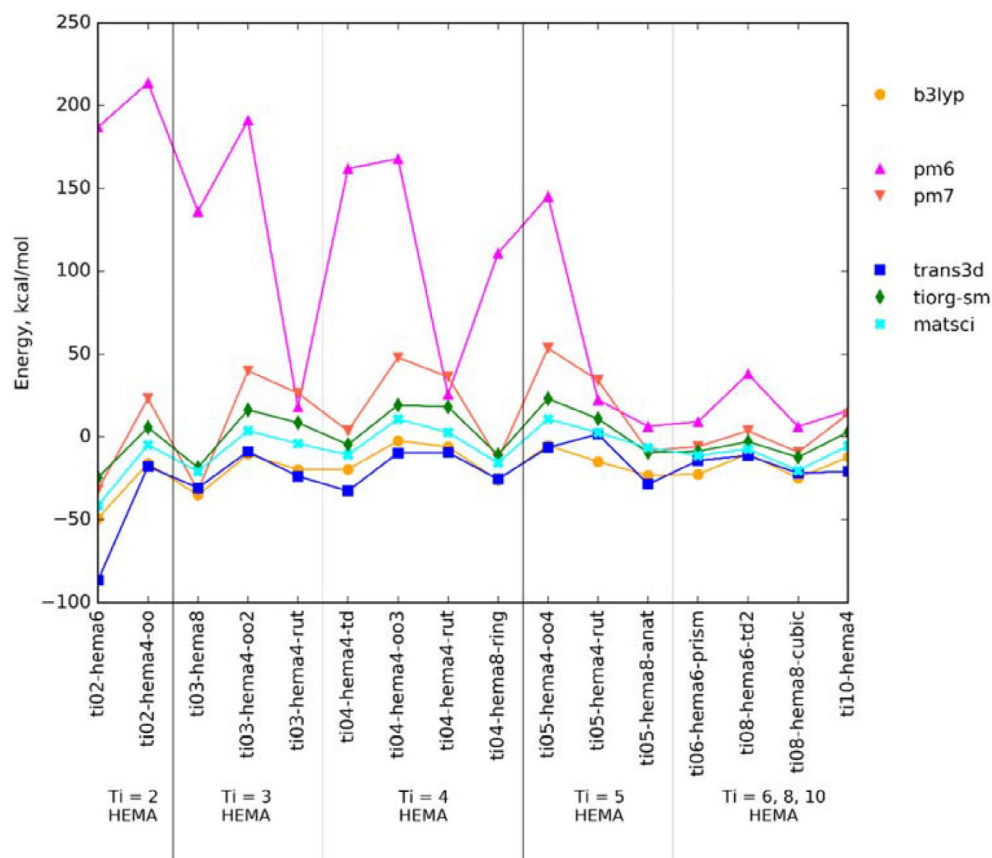


FIGURE 10 Energies of formation (represented by reaction (1)) for TiO₂/HEMA clusters

parameters differ from the *tiorg-smooth* and *trans3d* results, and the influence of the exact type of interactions is not as obvious as in the case of *tiorg-smooth* and *trans3d* sets.

3.5 | Adsorption on TiO₂ clusters

Adsorption energies of the CO molecule on the bare TiO₂ clusters (ΔE_{ads}) in the present study are calculated as:

$$\Delta E_{ads} = E_{complex} - (E_{cluster} + E_{CO}), \quad (2)$$

where $E_{complex}$ is the energy of adsorption complex, $E_{cluster}$ is the energy of TiO₂ cluster, and E_{CO} is the energy of a free CO molecule. The calculated adsorption energies and the optimized Ti···C/O distances are given in Table 4 in comparison with the previously published data and the results of the additional reference B3LYP/6-31G(d,p) calculations.

As is seen from the table, *tiorg-smooth* and *matsci* parameter sets well reproduce the adsorption energies, giving the reasonable values that are frequently close to the ranges obtained with different DFT approaches. Among these sets, the *tiorg-smooth* is in better agreement with the literature data, with typical deviations of only several kcal/mol. In comparison with B3LYP/6-31G(d,p) calculations, the *tiorg-smooth* set shows better performance for the adsorption complexes with Ti···O interactions, while deviations in the case of Ti···C complexes are larger. The deviations of *matsci* are somewhat worse; its values are typically overestimated, especially in the case of small-size systems, but more reliable for the Ti···C complexes. At the same time, the adsorption energies obtained with *trans3d* parameters poorly coincide with other sets and, moreover, frequently

TABLE 4 Energies and key geometry parameters for the CO adsorption on bare TiO₂ clusters calculated with DFT and different DFTB parameter sets

Complex	Adsorption energy, kcal/mol					Ti···C / Ti···O distance, Å				
	<i>b3lyp</i>	<i>tos</i>	<i>t3d</i>	<i>mtsc</i>	Previous studies	<i>b3lyp</i>	<i>tos</i>	<i>t3d</i>	<i>mtsc</i>	Previous studies
Carbon monoxide interacts with Ti with C atom										
ti10a_CO-0	-7.12	-2.59	-19.11	-11.53	-9.73 ... -3.12 ^a	2.423	3.036	2.520	2.523	2.443 ... 2.568 ^a
ti10a_CO-1	-17.09	-7.78	-3.05	-18.17	-5.18 ... -3.94 ^b	2.396	3.006	2.499	2.490	2.442 ... 2.603 ^b
ti10a_CO-2	-13.15	-4.68	-3.89	-20.13	-7.71 ... -5.70 ^c	2.399	3.023	2.503	2.499	2.396 ... 2.533 ^c
ti48b_CO-corner		-2.13	3.05	-8.77	-4.14 ... -1.62 ^d		3.041	2.525	2.526	2.326 ... 2.444 ^d
ti48b_CO-pit		-1.42	36.49	-0.54			3.418	2.568	3.614	
ti48b_CO-surface		-3.15	57.82	-0.05			3.033	2.542	2.544	
ti64a_CO-corner		-3.98	73.69	-7.21			3.027	2.529	2.533	
ti64a_CO-pit		-1.08	42.30	-0.52			3.145	2.574	3.763	
ti64a_CO-surface		-2.36	184.06	-4.34			3.039	2.542	2.542	
Carbon monoxide interacts with Ti with O atom										
ti10a_OC-0	-2.52	-2.37	-25.88	-12.52		3.722	2.885	2.573	2.267	
ti10a_OC-1	-10.38	-9.15	-6.81	-20.89		2.342	2.106	2.529	2.239	
ti10a_OC-2	-6.68	0.56	-8.06	-21.25		2.415	2.172	2.543	2.253	
ti48b_OC-corner		-2.03	-4.64	-9.90			2.888	2.570	2.268	
ti48b_OC-pit		-3.15	-39.72	-0.56			4.601	2.601	3.759	
ti48b_OC-surface		-2.68	49.91	-0.68			2.882	2.585	2.278	
ti64a_OC-corner		-3.32	2.91	-8.12			2.877	2.574	2.272	
ti64a_OC-pit		-0.82	31.52	-1.56			3.351	2.605	3.723	
ti64a_OC-surface		-2.20	108.41	-5.10			2.886	2.582	2.277	

Abbreviations: *b3lyp*, B3LYP/6-31G(d,p); *tos*, DFTB *tiorg-smooth* parameter set; *t3d*, DFTB *trans3d* parameter set; *mtsc*, DFTB *matsci* parameter set.

^aB3LYP with combined basis set.^[65]

^bB3LYP with combined basis set, values for the lowest levels of surface coverage.^[66]

^cPBE0 with combined basis set, values for the lowest levels of surface coverage.^[66]

^dB3LYP with combined basis set, values for the lowest levels of surface coverage.^[67]

^eExperimental value from temperature programmed desorption for adsorption energy for zero coverage limit.^[68]

TABLE 5 The comparison of energies and geometrical parameters for *trans3d* calculations with and without *tiorg-smooth* preoptimization

Structure	Total energy, eV			Ti–O _{all} distance, Å			O–Ti–O, °		
	<i>no preopt</i>	<i>preopt</i>	Δ	<i>no preopt</i>	<i>preopt</i>	Δ	<i>no preopt</i>	<i>preopt</i>	Δ
ti10a	–2156.5	–2155.5	–1.1	1.855	1.854	0.001	108.5	108.3	0.1
ti48b	–10 408.8	–10 399.6	–9.2	1.901	1.894	0.008	107.3	107.6	–0.2
ti64a	–13 895.6	–13 885.4	–10.2	1.908	1.898	0.009	107.3	107.4	–0.1
ti64a_OC-surf	–14 028.3	–14 028.8	0.5	1.903	1.902	0.001	107.2	107.2	0.0

Note: *no preopt*—start cluster geometry is taken from Reference 16. *preopt*—*tiorg-smooth*-optimized geometry is taken as start geometry. Δ—deviation between “*no preopt*” and “*preopt*.”

TABLE 6 Statistical analysis of the discrepancies between the DFTB results for the whole set of clusters

Property	Average values			Mean deviation		Mean absolute deviation	
	<i>tos</i>	<i>t3d</i>	<i>mtsc</i>	<i>t3d-tos</i>	<i>mtsc-tos</i>	<i>t3d-tos</i>	<i>mtsc-tos</i>
Structural properties							
Ti–O _{all} , Å	1.849 (1.831) [1.861]	1.870 (1.849) [1.883]	1.868 (1.859) [1.873]	0.021 (0.018) [0.022]	0.018 (0.028) [0.013]	0.023 (0.021) [0.024]	0.024 (0.028) [0.022]
Ti–O _{ino} , Å	1.867 (1.841) [1.880]	1.884 (1.852) [1.901]	1.875 (1.865) [1.880]	0.018 (0.011) [0.021]	0.008 (0.024) [0.000]	0.023 (0.021) [0.024]	0.025 (0.026) [0.024]
Ti–O _{org} , Å	1.811 (1.802) [1.815]	1.843 (1.834) [1.847]	1.858 (1.851) [1.861]	0.032 (0.032) [0.032]	0.047 (0.049) [0.046]	0.034 (0.032) [0.034]	0.048 (0.049) [0.047]
O–Ti–O, °	108.1 (108.6) [107.9]	108.3 (109.0) [107.9]	108.1 (108.4) [107.9]	0.2 (0.5) [0.0]	0.0 (–0.2) [0.1]	0.6 (0.8) [0.6]	0.5 (0.5) [0.5]
Ti–O–C, °	140.6 (141.1) [140.4]	109.9 (112.3) [108.7]	129.6 (129.9) [129.4]	–30.7 (–28.9) [–31.7]	–11.1 (–11.2) [–11.0]	30.7 (28.9) [31.7]	11.1 (11.2) [11.0]
Electronic properties							
E _{HOMO} , eV	–5.57 (–5.78) [–5.44]	–5.72 (–5.91) [–5.60]	–5.71 (–5.99) [–5.54]	–0.15 (–0.13) [–0.15]	–0.14 (–0.21) [–0.10]	0.26 (0.21) [0.29]	0.27 (0.23) [0.30]
E _{LUMO} , eV	–2.59 (–2.29) [–2.77]	–3.09 (–2.78) [–3.28]	–3.00 (–2.65) [–3.21]	–0.50 (–0.48) [–0.51]	–0.41 (–0.36) [–0.41]	0.53 (0.49) [0.56]	0.47 (0.39) [0.51]
Band gap, eV	2.98 (3.48) [2.67]	2.62 (3.14) [2.31]	2.71 (3.34) [2.33]	–0.35 (–0.35) [–0.36]	–0.26 (–0.14) [–0.34]	0.51 (0.43) [0.55]	0.43 (0.31) [0.51]
Dipole moment, D	–	–	–	0.42 (0.01) [0.66]	0.16 (0.09) [0.21]	3.55 (1.54) [4.75]	2.62 (1.42) [3.34]

Note: DFTB *tiorg-smooth* is reference method. Data represent values averaged among all clusters; among clusters studied at DFT, PM6, and PM7 levels (in parentheses); and among clusters studied at DFTB level only [in brackets].

Abbreviations: *tos*, *tiorg-smooth* parameter set; *t3d*, *trans3d* parameter set; *mtsc*, *matsci* parameter set.

give inadequate positive adsorption energy values. These positive energies, however, correspond to the stable coordinated structures, concluding that the positive energies originate from the strong electronic or structural rearrangements of the clusters during the coordination.

In order to elucidate the origin of such rearrangements, additional *trans3d* optimizations were performed using the *tiorg-smooth*-optimized initial geometries. It was found that the *trans3d* set is unreliable in describing the energy of the TiO_2 clusters. While bond lengths and angles between Ti and O atoms in the cluster are only slightly changed, the total energy of the cluster varies in the range of up to 10 eV. This instability is especially strong for the large bare TiO_2 clusters. In case of smaller clusters or the clusters with coordinated CO, the deviations are significantly lower. The full comparison is represented in Table 5.

It is interesting that *trans3d* shows better agreement with literature data for the structural parameters of the adsorption complexes, while *tiorg-smooth* and *matsci* results tend to overestimate the distance between the Ti atom and C atom of carbon monoxide. The largest deviation is obtained with the *tiorg-smooth* parameter set, with the distance overestimated by 0.6 Å. Discrepancies are smaller in the case of *matsci*, where the overestimation is about 0.2 to 0.3 Å. When the CO molecule is coordinated on the surface in the $\text{Ti}\cdots\text{O}$ mode, the deviations between the DFTB parameter sets are lower, and the underestimation is typical for the *tiorg-smooth* and *matsci* sets. Based on that, the most probable source of such deviations is the parametrization of repulsive $\text{Ti}\cdots\text{C}$ interactions, the strength of which increases from *trans3d* through *matsci* to *tiorg-smooth*. A good agreement between these sets was also found for valence angles $\text{Ti}-\text{O}-\text{C}$ (Figure 6). The relatively strong repulsion between Ti and C atoms in the case of *tiorg-smooth* makes the valence angle of $\text{Ti}-\text{O}-\text{C}$ more open and closer to the B3LYP values than in the cases of *matsci* and *trans3d*, where deviation from DFT is up to 30° .

Comparison between larger clusters calculated with different parameter sets. The clusters larger than the structures described above are impractical for treatment at the DFT level. In contrast, the DFTB method optimizes such structures easily. Therefore, we optimized 45 additional clusters having up to 448 atoms only with DFTB and compared the results obtained with *trans3d*, *tiorg-smooth*, and *matsci* parameters for all 72 structures. The structures of the 45 larger clusters are shown in Figure S1 of Supporting Information. Different types of TiO_2 structural patterns were simulated, including anatase- and rutile-like motifs described in the recent studies,^[16,52] as well as the TiO_2 /HEMA clusters surrounded by free HEMA molecules. The comparison between structural and electronic properties calculated with the *tiorg-smooth*, *trans3d*, and *matsci* parameter sets are shown in Table 6. DFTB with the *tiorg-smooth* parameter set is chosen as the reference method because the *tiorg-smooth* results are the closest to B3LYP in geometry.

As is evident from Table 6, deviations between results obtained with the different parameter sets are quite constant and do not dramatically change with cluster size growth. The parameter sets give similar values for almost all structural and electronic properties of large clusters except of valence angles, where *trans3d* and *matsci* give significant underestimation as described above. Dipole moment also differs, but the source of such discrepancies is in the geometry of clusters because the deviations in dipole moments are derivatives of differences in the structure (valence angle $\text{Ti}-\text{O}-\text{C}$).

4 | CONCLUSIONS

The comparison of the DFTB results of 27 bare TiO_2 and TiO_2 /organic clusters with the results of B3LYP calculations shows that all three DFTB parameter sets (*tiorg-smooth*, *trans3d*, and *matsci*) describe the structural and electronic properties of clusters (HOMO-LUMO gap, ionization potential, and dipole moment) at the level that is comparable to the DFT calculations. It is noticeable that DFTB demonstrates the deviations from the DFT values, which are only slightly dependent on the cluster size or their structure. The electronic parameters at the DFTB level are closer to experimental data than the DFT results regardless of the model size. These properties differ remarkably in the considered structures, and the convergence of these parameters with the cluster size is quite slow and nonmonotonous. From this point of view, the DFTB method has an advantage over DFT because it allows one to consider structures whose size is close to experimentally synthesized particles. At the same time, the semiempirical methods demonstrate noticeable deviations from the DFT calculations for the small clusters containing fewer than seven Ti atoms.

In comparison with the PM6 and PM7 methods, DFTB demonstrates better performance at describing thermodynamic properties, as well as in reproducing their structures. The corrected *tiorg-smooth* parameter set has better performance for the estimation of structural parameters of TiO_2 /organic clusters and perfectly reproduces B3LYP structures for such clusters. For the CO adsorption complexes, *tiorg-smooth* gives more realistic adsorption energies, although it overestimates the coordination bond lengths. The *trans3d* set better reproduces the energies of composite material formation in polycondensation reactions, as well as important geometrical parameters for the bare TiO_2 clusters interacting with molecules, including carbon atoms. However, *trans3d* should be used with caution for the thermodynamic estimations of large bare TiO_2 clusters and for the description of adsorption processes. The *matsci* set is slightly better than the PM7 method in the structural calculations and slightly worse than *trans3d* in the estimations of thermodynamics of polycondensation. The *matsci* set properly reproduces structural parameters and adsorption energies, which makes it another method of choice in adsorption calculations due to its better performance in the structural parameters in the case of the intermolecular $\text{Ti}\cdots\text{C}$ interactions than the *tiorg-smooth* parameter set. All three DFTB parameters sets have similar accuracy in the calculations of electronic properties. Stability and robustness of the DFTB method are confirmed by the calculations of large (up to 448 atoms) TiO_2 clusters.

ACKNOWLEDGMENT

NIST Raritan Cluster was used to perform Gaussian16 calculations. DFTB calculations were performed using the facilities of Bremen Center for Computational Material Science (BCCMS) and Lobachevsky Supercomputer.

AUTHOR CONTRIBUTIONS

Vladimir S. Naumov: Conceptualization; data curation; formal analysis; investigation; project administration; software; visualization; writing-original draft; funding acquisition. **Anastasiia S. Loginova:** Funding acquisition; investigation. **Alexander A. Avdoshin:** Data curation; visualization. **Stanislav K. Ignatov:** Conceptualization; funding acquisition; resources; supervision; writing-review and editing. **Alexey V. Mayorov:** Investigation; resources. **Bálint Aradi:** Investigation; software; supervision; writing-review and editing. **Thomas Frauenheim:** Funding acquisition; resources; supervision.

ORCID

Vladimir S. Naumov  <https://orcid.org/0000-0003-0035-3028>

Stanislav K. Ignatov  <https://orcid.org/0000-0002-6039-3905>

REFERENCES

- [1] M. Jakob, H. Levanon, P. V. Kamat, *Nano Lett.* **2003**, *3*, 353.
- [2] M. Es-Souni, M. Es-Souni, S. Habouti, N. Pfeiffer, A. Lahmar, M. Dietze, C.-H. Solterbeck, *Adv. Funct. Mater.* **2010**, *20*, 377.
- [3] M. S. Hamdy, W. H. Saputera, E. J. Groenen, G. Mul, *J. Catal.* **2014**, *310*, 75.
- [4] H.-J. Zhai, L.-S. Wang, *J. Am. Chem. Soc.* **2007**, *129*, 3022.
- [5] R. Sánchez-de-Armas, J. Oviedo López, M. A. San-Miguel, J. F. Sanz, P. Ordejón, M. Pruneda, *J. Chem. Theory Comput.* **2010**, *6*, 2856.
- [6] R. Sánchez-de-Armas, M. A. San-Miguel, J. Oviedo, A. Márquez, J. F. Sanz, *Phys. Chem. Chem. Phys.* **2011**, *13*, 1506.
- [7] C. I. Oprea, P. Panait, F. Cimpoesu, M. Ferbinteanu, M. A. Gîrțu, *Materials (Basel)* **2013**, *6*, 2372.
- [8] C. Oprea, P. Panait, J. Lungu, D. Stamate, A. Dumbrava, C. Fanica, M. Girtu, *Int. J. Photoenergy* **2013**, *2013*, 1.
- [9] C. I. Oprea, M. A. Gîrțu, *Nanomaterials* **2019**, *9*, 357.
- [10] P. Persson, M. J. Lundqvist, *J. Phys. Chem. B* **2005**, *109*, 11918.
- [11] M. J. Lundqvist, M. Nilsing, P. Persson, S. Lunell, *Int. J. Quantum Chem.* **2006**, *106*, 3214.
- [12] M. J. Lundqvist, M. Nilsing, S. Lunell, B. Åkermark, P. Persson, *J. Phys. Chem. B* **2006**, *110*, 20513.
- [13] M. Pastore, F. De Angelis, *Phys. Chem. Chem. Phys.* **2012**, *14*, 920.
- [14] J. Chen, F.-Q. Bai, J. Wang, L. Hao, Z.-F. Xie, Q.-J. Pan, M.-X. Song, *Dyes Pigm.* **2012**, *94*, 459.
- [15] M. Gałyńska, P. Persson, *Int. J. Quantum Chem.* **2013**, *113*, 2611.
- [16] M. Chen, D. A. Dixon, *Nanoscale* **2017**, *9*, 7143.
- [17] L. A. Fredin, K. Wärnmark, V. Sundström, P. Persson, *ChemSusChem* **2016**, *9*, 667.
- [18] F. De Angelis, A. Tilocca, A. Selloni, *J. Am. Chem. Soc.* **2004**, *126*, 15024.
- [19] F. De Angelis, S. Fantacci, A. Selloni, M. K. Nazeeruddin, M. Grätzel, *J. Phys. Chem. C* **2010**, *114*, 6054.
- [20] F. De Angelis, S. Fantacci, E. Mosconi, M. K. Nazeeruddin, M. Grätzel, *J. Phys. Chem. C* **2011**, *115*, 8825.
- [21] Y.-F. Li, Z.-P. Liu, *J. Am. Chem. Soc.* **2011**, *133*, 15743.
- [22] T. Homann, T. Bredow, K. Jug, *Surf. Sci.* **2004**, *555*, 135.
- [23] A. V. Vorontsov, *Catal. Today* **2015**, *252*, 168.
- [24] A. V. Vorontsov, P. G. Smirnotis, *J. Photochem. Photobiol., A* **2018**, *363*, 51.
- [25] L. Rottmannova, J. Rimarcik, T. Vesely, E. Klein, V. Lukes, *Acta Chim. Slovaca* **2010**, *3*, 12.
- [26] D. Mendoza-Espinosa, A. Alvarez-Hernández, D. Angeles-Beltrán, G. E. Negrón-Silva, O. R. Suárez-Castillo, J. M. Vásquez-Pérez, *Inorg. Chem.* **2017**, *56*, 2092.
- [27] G. Liu, Y. Xiong, R. Gou, C. Zhang, *J. Phys. Chem. C* **2019**, *123*, 16565.
- [28] M. Kar, R. Sarkar, S. Pal, P. Sarkar, *J. Phys. Chem. C* **2019**, *123*, 5303.
- [29] A. Buin, S. Consta, T.-K. Sham, *J. Phys. Chem. C* **2011**, *115*, 22257.
- [30] Y. Ding, Y. Wang, *J. Phys. Chem. C* **2014**, *118*, 4509.
- [31] A. S. Barnard, G. Opletal, S. L. Y. Chang, *J. Phys. Chem. C* **2019**, *123*, 11207.
- [32] M. Van den Bossche, *J. Phys. Chem. A* **2019**, *123*, 3038.
- [33] A. K. Das, M. Meuwly, *J. Phys. Chem. B* **2017**, *121*, 9024.
- [34] F. Bi, S. Markov, R. Wang, Y. Kwok, W. Zhou, L. Liu, X. Zheng, G. Chen, C. Yam, *J. Phys. Chem. C* **2017**, *121*, 11151.
- [35] S. Mukherjee, C. Liu, E. Jakubikova, *J. Phys. Chem. A* **2018**, *122*, 1821.
- [36] G. Zheng, H. A. Witek, P. Bobadova-Parvanova, S. Irlé, D. G. Musaev, R. Prabhakar, K. Morokuma, M. Lundberg, M. Elstner, C. Köhler, T. Frauenheim, *J. Chem. Theory Comput.* **2007**, *3*, 1349.
- [37] G. Dolgonos, B. Aradi, N. H. Moreira, T. Frauenheim, *J. Chem. Theory Comput.* **2010**, *6*, 266.
- [38] R. Luschtinetz, J. Frenzel, T. Milek, G. Seifert, *J. Phys. Chem. C* **2009**, *113*, 5730.
- [39] S. Gemming, A. N. Enyashin, J. Frenzel, G. Seifert, *Int. J. Mater. Res.* **2010**, *101*, 758.
- [40] D. Selli, G. Fazio, C. Valentin, *Catalysts* **2017**, *7*, 357.
- [41] D. Selli, G. Fazio, G. Seifert, C. Di Valentin, *J. Chem. Theory Comput.* **2017**, *13*, 3862.
- [42] D. V. Ludin, S. D. Zaitsev, Y. L. Kuznetsova, A. V. Markin, A. E. Mochalova, E. V. Salomatina, *J. Polym. Res.* **2017**, *24*, 117.
- [43] E. V. Salomatina, A. S. Loginova, S. K. Ignatov, A. V. Knyazev, I. V. Spirina, L. A. Smirnova, *J. Inorg. Organomet. Polym. Mater.* **2016**, *26*, 1280.

- [44] A. S. Loginova, S. K. Ignatov, E. P. Chukhmanov, E. V. Salomatina, L. A. Smirnova, *Comput. Theor. Chem.* **2017**, *1118*, 1.
- [45] O. A. Ryabkova, E. Salomatina, A. V. Knyazev, L. Smirnova, *Inorg. Mater.* **2019**, *10*, 431.
- [46] B. Aradi, B. Hourahine, T. Frauenheim, *J. Phys. Chem. A* **2007**, *111*, 5678.
- [47] J. J. Stewart, *J. Mol. Model.* **2007**, *13*, 1173.
- [48] J. J. P. Stewart, *J. Mol. Model.* **2013**, *19*, 1.
- [49] M. J. T. Frisch, G. W. H. B. Schlegel, G. E. Scuseria, M. A. Robb, J. R. Cheeseman, J. A. Montgomery Jr., T. Vreven, K. N. Kudin, J. C. Burant, et al., *Gaussian 09*, Gaussian, Inc., Wallingford, CT **2004**.
- [50] M.J. Frisch, G.W. Trucks, H.B. Schlegel, G.E. Scuseria, M.A. Robb, J.R. Cheeseman, G. Scalmani, V. Barone, G.A. Petersson, H. Nakatsuji, X. Li, M. Caricato, A.V. Marenich, J. Bloino, B.G. Janesko, R. Gomperts, B. Mennucci, H.P. Hratchian, J.V. Ortiz, A.F. Izmaylov, J.L. Sonnenberg, D. Williams, F. Ding, F. Lipparini, F. Egidi, J. Goings, B. Peng, A. Petrone, T. Henderson, D. Ranasinghe, V.G. Zakrzewski, J. Gao, N. Rega, G. Zheng, W. Liang, M. Hada, M. Ehara, K. Toyota, R. Fukuda, J. Hasegawa, M. Ishida, T. Nakajima, Y. Honda, O. Kitao, H. Nakai, T. Vreven, K. Throssell, J.A. Montgomery Jr., J.E. Peralta, F. Ogliaro, M.J. Bearpark, J.J. Heyd, E.N. Brothers, K.N. Kudin, V.N. Staroverov, T.A. Keith, R. Kobayashi, J. Normand, K. Raghavachari, A. P. Rendell, J.C. Burant, S.S. Iyengar, J. Tomasi, M. Cossi, J.M. Millam, M. Klene, C. Adamo, R. Cammi, J.W. Ochterski, R.L. Martin, K. Morokuma, O. Farkas, J.B. Foresman, D.J. Fox, *Gaussian 16 Rev. C.01*, Gaussian, Inc., Wallingford, CT **2016**.
- [51] L. X. Chen, T. Rajh, Z. Wang, M. C. Thurnauer, *J. Phys. Chem. B* **1997**, *101*, 10688.
- [52] K. C. Ko, S. T. Bromley, J. Y. Lee, F. Illas, *J. Phys. Chem. Lett.* **2017**, *8*, 5593.
- [53] L. X. Chen, T. Rajh, W. Jäger, J. Nedeljkovic, M. C. Thurnauer, *J. Synchrotron Radiat.* **1999**, *6*, 445.
- [54] E. P. Meagher, G. A. Lager, *The Canadian Mineralogist* **1979**, *17*, 77.
- [55] J. K. Burdett, T. Hughbanks, G. J. Miller, J. W. Richardson, J. V. Smith, *J. Am. Chem. Soc.* **1987**, *109*, 3639.
- [56] S. Kashiwaya, J. Morasch, V. Streibel, T. Toupance, W. Jaegermann, A. Klein, *Surfaces* **2018**, *1*, 73.
- [57] F. C. Marques, J. J. Jasieniak, *Appl. Surf. Sci.* **2017**, *422*, 504.
- [58] Y. Nakano, T. Morikawa, T. Ohwaki, Y. Taga, *Chem. Phys.* **2007**, *339*, 20.
- [59] H. Wu, L. S. Wang, *J. Chem. Phys.* **1997**, *107*, 8221.
- [60] S. Valencia, J. Marín, G. Restrepo, *Open Mater. Sci. J.* **2010**, *4*, 9.
- [61] G. Xiong, R. Shao, T. C. Droubay, A. G. Joly, K. M. Beck, S. A. Chambers, W. P. Hess, *Adv. Funct. Mater.* **2007**, *17*, 2133.
- [62] D. Bégué, I. Baraille, P. A. Garrain, A. Dargelos, T. Tassaing, *J. Chem. Phys.* **2010**, *133*, 034102.
- [63] E. V. Salomatina, N. M. Bityurin, M. V. Gulenova, T. A. Gracheva, M. N. Drozdov, A. V. Knyazev, K. V. Kir'yanov, A. V. Markin, L. A. Smirnova, *J. Mater. Chem. C* **2013**, *1*, 6375.
- [64] M. Elstner, D. Porezag, G. Jungnickel, J. Elsner, M. Haugk, T. Frauenheim, S. Suhai, G. Seifert, *Phys. Rev. B* **1998**, *58*, 7260.
- [65] R. Wanbayor, V. Ruangpornvisuti, *Mater. Chem. Phys.* **2010**, *124*, 720.
- [66] L. Mino, A. M. Ferrari, V. Lacivita, G. Spoto, S. Bordiga, A. Zecchina, *J. Phys. Chem. C* **2011**, *115*, 7694.
- [67] J. Scaranto, S. Giorgianni, *Mol. Simul.* **2013**, *39*, 245.
- [68] M. Setvin, M. Buchholz, W. Hou, C. Zhang, B. Stöger, J. Hulva, T. Samschitz, X. Shi, J. Pavelec, G. S. Parkinson, M. Xu, Y. Wang, M. Schmid, C. Wöll, A. Selloni, U. Diebold, *J. Phys. Chem. C* **2015**, *119*, 21044.
- [69] T. Yanai, D. P. Tew, N. C. Handy, *Chem. Phys. Lett.* **2004**, *393*, 51.

SUPPORTING INFORMATION

Additional supporting information may be found online in the Supporting Information section at the end of this article.

How to cite this article: Naumov VS, Loginova AS, Avdoshin AA, et al. Structural, electronic, and thermodynamic properties of TiO₂/organic clusters: performance of DFTB method with different parameter sets. *Int J Quantum Chem.* 2020;e26427. <https://doi.org/10.1002/qua.26427>